IEEE Access
Multidisciplinary | Rapid Review | Open Access Journal

Received August 13, 2019, accepted September 1, 2019, date of publication September 6, 2019, date of current version September 20, 2019.

Digital Object Identifier 10.1109/ACCESS.2019.2939847

Robust Beamforming-Aided Signal Recovery for MIMO VLC System With Incomplete Channel

HUIQIN DU[1,2], (Member, IEEE), CHONG ZHANG[1], AND ZUJIAN WU[3]

[1]College of Information Science and Technology, Jinan University, Guangzhou 510632, China
[2]National Mobile Communications Research Laboratory, Southeast University, Nanjing 210009, China
[3]Jinan University-University of Birmingham Joint Institute (J-BJI), Jinan University, Guangzhou 510632, China

Corresponding author: Huiqin Du (thuiqin.du@jnu.edu.cn)

The work of H. Du and C. Zhang was supported in part by the National Natural Science Foundation of China under Grant 61401178, and in part by the Open Research Fund of the National Mobile Communications Research Laboratory, Southeast University, under Grant 2017D12. The work of Z. Wu was supported by the National Natural Science Foundation of China under Grant 61602209.

ABSTRACT Visible light communication (VLC) based on light emitting diodes (LEDs) has attracted much attention because of its high data rate and energy efficiency. However, the shadowing caused by any mobile obstacles could block the light-of-sight (LoS) link which may have a dramatical effect on the indoor VLC channel state information (CSI). Instead of investigating the shadowing channel characteristics, we model the link blockages as the incomplete channel matrix with sparse missing elements and reconstruct the transmitted signal by the ℓ_0-minimization with additional constraint on shadowing loss. However, the indoor VLC channel is highly correlated especially in cases with small emitter separation. To further improve the accuracy performance, we design the transmit beamforming to reduce the total coherence. Simulation results illustrate the effectiveness of the proposed signal recovery algorithm with incomplete channel and further significant enhancement via the proposed beamforming design.

INDEX TERMS Visible light communication, signal recovery, beamforming, transmit coherence, incomplete channel.

I. INTRODUCTION

The VLC could offer a strong wireless communication alternative to radio frequency (RF) used in indoor communication because of its advantages such as cost-effective, high security, license-free and immunity to RF interference [1], [2]. In general, the system performance of VLC depends heavily on perfect CSI, which however is not available due to feedback delays, quantization errors, channel estimated errors in practice. Beside the invertible channel imperfections, the communications link may experience temporary blockage or shadowing in dynamic environments (i.e. mobile people and obstacles), which may lead to severe degradation on system performance.

Many effects have been made against shadowing effect in terms of the system configuration [3], [4], the channel modeling [5]–[9]. The radiation angle at the transmitter is configured which can guarantee the low probability of shadowing with negligible power penalty caused by shadowing [3], while the number of LED is designed to provide robustness against shadowing over the downlink transmission [4]. Besides the system configuration, the statistical properties of the shadowing are investigated. For instance, under the assumption of ideal Lambertian LED source, the random shadowing is represented as a weighted Possion process [7]. Considering the small number of the obstacles, the obstacle is modeled as a convex hull and the beam steering technology is designed to detect the obstacles based on the division of the illumination area [9]. Moreover, the tray tracking is another approach including the triangulation algorithm [10] and probabilistic filtering approach [11], under the assumption that one lamp is shadowed. In realistic VLC scenario, the blockage or shadowing would be at random positions with any shape, size and number, resulting in the incomplete channel which may be changed dramatically. Therefore, the conventional channel uncertainty models such as the statistical error and the deterministic error [12]–[16] cannot be used to present the shadowing effect, which motivates us to propose a new channel uncertainty model for link blockages.

The associate editor coordinating the review of this manuscript and approving it for publication was Danping He.

Recently, generalized spatial modulation (GenSM) that takes full advantage of the spatial domain to transmit more information is extended to the VLC system. The combination can improve its spectral efficiency and energy efficiency [17]–[21], in which some of transmit LEDs are activated at the same time to transmit information, leading the sparsity of transmitted signal. Due to its sparsity, the transmitted signal can be recovered via ℓ_0-minimization under the compress sensing (CS) frameworks, such as matching pursuit (MP) [22], orthogonal matching pursuit (OMP) [23], compressive sampling matching pursuit (CoSaMP) [24], and $\ell_0$smooth-norm (SL0) [25]. More specifically, the MP algorithm has a slow convergence speed and high computation complexity, while the OMP algorithm improves the convergence speed but limited tolerance on the channel errors. Meanwhile, due to the slow continuous function, the CoSaMP and SL0 algorithms can only achieve inaccurate recovery. The ℓ_0-norm problem can be further solved by alternating direction method of multipliers (ADMM) or fast iterative shrinkage thresholding algorithm (FISTA). It is worthy to note that most of the aforementioned CS-based optimization problems only involve one observation constraint under noiseless scenario, i.e. the perfect measurement matrix (or channel matrix).

Moreover, due to the small emitter separation of the PDs, the indoor VLC channel responses among the users could be highly correlated, handicapping the performance of the aforementioned signal recovery. Besides the development on physical devices [26], [27], the precoding approach is introduced to eliminate channel correlation [28]–[31]. More specifically, the correlated VLC indoor channel is decomposed into several independent parallel sub-channels through the singular value decomposition (SVD)-based precoding with low channel coherence achieved [28], [29]. Moreover, the zero-forcing (ZF) precoding method chooses the transmission mode according to the ratio of the maximum eigenvalue to the sum of all eigenvalues of the channel. The channel correlation can be significantly reduced, especially when the maximum eigenvalue of the channel correlation matrix accounts for a large proportion of the sum of all eigenvalues [30], [31]. However, the aforementioned schemes are designed based on perfect CSI, which cannot be directly implemented in the shadowing scenario where the channel matrix might be ill-conditioned or not full rank due to the link blockages.

In this work, we consider an indoor multiple-input-multiple-output (MIMO) system in which the LEDs cover the surface of the ceiling. Considering the dynamical shadowing caused by the movement of people and obstacles, we model the LoS links as the incomplete channel matrix in which the missing elements present the link blockages. Under the incomplete channel matrix, the ℓ_0-minimization is introduced to reconstruct the signal with additional constraint to limit the shadowing effect. Further approximation of the $\ell_1 - \ell_1$ minimization is developed and the optimum solution is achieved via ADMM algorithm iteratively. Moreover,

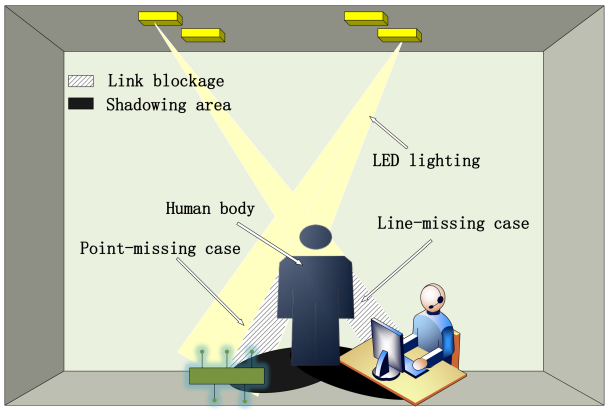

FIGURE 1. Shadowing effect caused by obstacle in MIMO VLC system.

it is noted that the highly-correlated indoor VLC channel may result in large sum-of-square error (SSE) of recovered signals, which motivates us to reduce the channel coherence further. According to the restricted isometry property (RIP) constraint of CS framework, it indicates that the sufficiently low channel coherence guarantees the exact recovery of the sparse signal vector [32]–[34]. We are inspired to design the transmit beamforming to reduce the total coherence in which the coherence of the equivalent channel is minimized. Simulation results illustrate the effectiveness of the proposed signal recovery algorithm with incomplete channel and the significant improvement by minimizing the total coherence. The main contributions of this paper can be summarized as follows,

- We propose the incomplete channel model to present the dynamical link blockages, in which the random-selected missing elements indicate the temporarily blocked transmission links.
- We introduce the ℓ_0-minimization to reconstruct the transmitted GenSM signals with additional constraint that eliminates the shadowing effect, which is further approximated as the $\ell_1 - \ell_1$ optimization and solved by ADMM algorithm.
- We further design the transmit beamforming to minimize the total coherence of the equivalent channel and improve the recovery accuracy of the transmitted signal.

The remainder of the paper is organized as follows. Section II presents the incomplete channel model and formulates the ℓ_0-minimization problem. The proposed signal recovery problem is solved in Section III with further improvement on beamforming design in Section IV. Simulation results are presented in Section V, followed by a conclusion in Section VI.

II. SYSTEM MODEL AND PROBLEM FORMULATION

We consider an optical wireless MIMO system with LED arrays, in which N_T identical LEDs are utilized for illumination and data transmission and N_R photodetectors (PDs) installed. We assume the Lambertian radiation pattern for the LEDs, and only consider the LoS between the LEDs and

PDs. The corresponding LoS channel matrix $\mathbf{H} \in \mathbb{R}^{N_R \times N_T}$ between the transmitters and receivers can be given by

$$\mathbf{H} = \begin{bmatrix} h_{11} & h_{12} & \dots & h_{1N_T} \\ h_{21} & h_{22} & \dots & h_{2N_T} \\ \vdots & \vdots & \vdots & \vdots \\ h_{N_R1} & h_{N_R2} & \dots & h_{N_RN_T} \end{bmatrix}, \tag{1}$$

where each element h_{ij} of $\mathbf{H}$ is defined as the channel gain between the i-th receiver and j-th transmitter, that is,

$$h_{ij} = \begin{cases} \frac{A_i}{d_{ij}^2} R_0(\phi_{ij}) \cos(\varphi_{ij}) & 0 \le \varphi_{ij} \le \varphi_c \\ 0 & \varphi_{ij} > \varphi_c, \end{cases} \tag{2}$$

with the distance d_{ij} between the i-th receiver and j-th transmitter, the emission angle ϕ_{ij}, the incidence angle of the light φ_{ij}, the collection area of the i-th receiver A_i and the receiver field of view (FOV) φ_c. The $R_0(\phi)$ is given by

$$R_0(\phi) = [(m+1)/2\pi] cos^m(\phi), \tag{3}$$

where m is the order of Lambertian emission.

In this work, we consider the practical scenario that contains certain obstacles, such as in the furniture equipped office room or corridor, instead of empty room. To simplify the model, the rays are assumed to be absorbed after meeting the obstacle while they are scattered after meeting the walls, ceiling, and floor. Thus, the rays transmitted from the light source that are blocked by the obstacle cannot be received. With the link blockages, the channel could be dramatically degraded, followed with total received power reduced at PDs. Hence, a proper channel model that includes obstacles would be in great need for high reliable VLC system design. The standard channel uncertainty models, such as the norm-bounded error [12]–[14] and statistical error [15], [16], cannot be implemented in the shadowing scenario. The obstacle, such as, human body is modeled in the form of a rectangular shape object [5]–[9]. It shows that the corresponding positions of the luminance level drop to very low where the normalized received optical power is distributed along the receiver plan with obstacles [5]. Moreover, [9] further demonstrates that the blocked ray modeled as zero is valid when the receiver at PD is inside the shadowing hull of the obstacle. Therefore, when the receiver at PD is inside the shadowing area of the obstacles, the corresponding link is blocked, and the corresponding elements in channel matrix is reasonable to be zero. Consequently, the channel matrix is modeled as two parts, that is, incomplete matrix that represents the link-blocked channel and shadowing matrix that represents the missing elements due to the obstacles. Considering the obstacles would be at random positions with any shape and size, we model the shadowing as random missing elements, and the perfect channel $\mathbf{H}$ can be represented as

$$\mathbf{H} = \hat{\mathbf{H}} + \mathbf{\Delta}, \tag{4}$$

where $\hat{\mathbf{H}} \in \mathbb{R}^{N_R \times N_T}$ is the incomplete channel with sparse missing elements, and the shadowing channel $\mathbf{\Delta} \in \mathbb{R}^{N_R \times N_T}$ contains a lot of zeros and only a few nonzero elements where the non-zeros present the missing elements due to the blockage of the links. More specifically, when the receiver at PD is inside the shadowing area of the obstacles, the corresponding link is blocked, that is,

1) Point-missing case in which total k_2 ($k_2 \le N_T \times N_R$) elements are selected to be non-zero. For instance, when the shadowing projection of the obstacle on the PD is relatively small compared with the receiver at PD, only the link between j-th transmitter and the i-th receiver is blocked, that is, the (i, j)-th element of Δ is non-zero.
2) Line-missing case in which total k_1 ($k_1 \le N_T$ or N_R) row or column are randomly set to be non-zero. For instance, when the shadowing projection of the obstacle on the PD is relatively large compared with the receiver at PD, all links to the i-th receiver is blocked, that is, the i-th column of Δ is non-zero.

With GenSM, some of the LEDs are activated at the same time to transmit information and the combinations of the indices of the activated LEDs are utilized to transmit spatial-domain information as well. According to the principle of GenSM [17]–[21], the transmitted signal $\mathbf{x} \in \mathbb{R}^{N_T \times 1}$ contains L non-zero elements, such as,

$$\mathbf{x} = \mathbf{W}\mathbf{s} = [0, \dots, s_1, \dots, s_k, s_{k+1}, \dots, s_L, \dots, 0]^T, \tag{5}$$

where $\mathbf{s} \in \mathbb{R}^{L \times 1}$ ($L < N_T$) is the intended modulated signal, and the precoder $\mathbf{W} \in \mathbb{R}^{N_T \times L}$ works as antenna selection under the GenSM scheme, i.e. $\|\mathbf{W}_i\|_2 = 1$. Note that, the transmitted signal $\mathbf{x}$ is sparse and zero-dominant. Moreover, followed the assumption in [17], [19], the channel impulse responses are estimated under the downlink of time-division duplexing (TDD)-based architectures, and the L-length intended symbols $\mathbf{s}$ are transmitted through the selected antenna via the precoder matrix $\mathbf{W}$. Let $\boldsymbol{\delta} = \Delta\mathbf{x} \in \mathbb{R}^{N_R \times 1}$, the received signal vector $\mathbf{y} \in \mathbb{R}^{N_R \times 1}$ can be written as

$$\mathbf{y} = \mathbf{H}\mathbf{x} + \mathbf{n} = \left(\hat{\mathbf{H}} + \Delta\right)\mathbf{x} + \mathbf{n} = \hat{\mathbf{H}}\mathbf{x} + \boldsymbol{\delta} + \mathbf{n}, \tag{6}$$

where $\mathbf{n} \in \mathbb{R}^{N_R \times 1}$ is the noise vector that follows the zero-mean Gaussian distribution, i.e. $\mathbf{n} \sim \mathcal{N}(\mathbf{0}, \sigma_e^2\mathbf{I})$. Note that, the vector $\boldsymbol{\delta}$ would be sparse because of the sparsity of the transmitted signal in (4) and (5).

We propose the CS-based framework to reconstruct the transmitted signal by utilizing the sparsity of $\boldsymbol{\delta}$ and $\mathbf{x}$, that is,

$$\min_{\mathbf{x}} \quad \|\mathbf{x}\|_0 \tag{7a}$$

$$\text{s.t. } \|\boldsymbol{\delta}\|_0 \le \tau \quad \|\mathbf{y} - \hat{\mathbf{H}}\mathbf{x} - \boldsymbol{\delta}\|_2^2 \le N_R\sigma_e^2, \tag{7b}$$

where the additional constraint $\|\boldsymbol{\delta}\|_0 \le \tau$ strives to limit the shadowing effect with the sparsity level $\tau > 0$. Due to the $\|\cdot\|_0$ terms, (7) is NP-hard, and the ℓ_1-norm is introduced as an alternative surrogate. As the result, the underlying

problem (7) can be further approximated as

$$\min_{\mathbf{x}} \ \|\mathbf{x}\|_1 \tag{8a}$$

$$\text{s.t. } \|\boldsymbol{\delta}\|_1 \le \tau \quad \|\mathbf{y} - \hat{\mathbf{H}}\mathbf{x} - \boldsymbol{\delta}\|_2^2 \le N_R\sigma_e^2, \tag{8b}$$

which can be cast as a second order cone programming problem and could be solved via interior point methods.

III. SIGNAL RECOVERY VIA ADMM WITH INCOMPLETE CHANNEL

The aforementioned optimization problem (8) can be solved via standard CVX toolbox. However, the incomplete channel is ill-conditioned due to the shadowing loss, which may lead to inaccurate signal recovery. Moreover, the infeasible solution may be easily achieved because of the improper specified boundaries, especially when the boundary is specified empirically. The ℓ_1-regularization is one of the effective approaches to jointly optimize multiple variables, such as

$$\min_{\mathbf{x}} \ \| \mathbf{y} - \hat{\mathbf{H}}\mathbf{x} - \boldsymbol{\delta} \|_2^2 + \lambda_1 \| \mathbf{x} \|_1 + \lambda_2 \| \boldsymbol{\delta} \|_1, \tag{9}$$

where the first term prompts the noise sensitivity to be small, the second term encourages a sparse solution, and the regularization parameters λ_1 and λ_2 ($\lambda_1 + \lambda_2 = 1$) weight the recovery accuracy and noise sensitivity, respectively. However, the underlying problem includes only one variable $\mathbf{x}$ and its three terms cannot be minimized separately. Therefore, the ADMM algorithm that blends the decomposability of dual ascent with the superior convergence properties of the method of multipliers is introduced to offer a linear convergence rate and a natural extension to a decentralized implementation [35]. By introducing an intermediate variable $\mathbf{z} \in \mathbb{R}^{N_R \times 1}$ as bridge parameter to establish consensus among $\mathbf{x}$, the problem (9) can be reformulated as

$$\min_{\mathbf{x},\mathbf{z},\boldsymbol{\delta}} \ \| \mathbf{y} - \hat{\mathbf{H}}\mathbf{x} - \boldsymbol{\delta} \|_2^2 + \lambda_1 \| \mathbf{z} \|_1 + \lambda_2 \| \boldsymbol{\delta} \|_1, \tag{10a}$$

$$\text{s.t. } \mathbf{z} = \mathbf{x}. \tag{10b}$$

The corresponding augmented Lagrangian function over $\mathbf{x}$, $\mathbf{z}$ and $\boldsymbol{\delta}$ can be written as,

$$\mathcal{L}_\rho(\mathbf{z}, \mathbf{x}, \boldsymbol{\delta}, \Theta) = \| \mathbf{y} - \hat{\mathbf{H}}\mathbf{x} - \boldsymbol{\delta} \|_2^2 + \lambda_1 \| \mathbf{z} \|_1 + \lambda_2 \| \boldsymbol{\delta} \|_1 + \rho/2 \| \mathbf{z} - \mathbf{x} + \Theta/\rho \|_2^2, \tag{11}$$

where $\Theta \in \mathbb{R}^{N_R \times 1}$ is a dual variable and $\rho > 0$ is a positive penalty parameter. In each iteration of ADMM, we perform alternating minimization of the augmented Lagrangian over $\mathbf{x}$, $\mathbf{z}$ and $\boldsymbol{\delta}$ by taking $\partial\mathcal{L}/\partial\mathbf{x} = 0$, $\partial\mathcal{L}/\partial\mathbf{z} = 0$ and $\partial\mathcal{L}/\partial\boldsymbol{\delta} = 0$, respectively. More specifically, each variable is updated by

$$\mathbf{x}^{k+1} = (2\hat{\mathbf{H}}^T\hat{\mathbf{H}} + \rho\mathbf{I})^{-1}(\rho\mathbf{z}^k + 2\hat{\mathbf{H}}^T(\mathbf{y} - \boldsymbol{\delta}^k) + \boldsymbol{\Theta}^k), \tag{12a}$$

$$\mathbf{z}^{k+1} = shrink(\mathbf{x}^{k+1} - \frac{\boldsymbol{\Theta}^k}{\rho}, \frac{\lambda_1}{\rho}), \tag{12b}$$

$$\boldsymbol{\delta}^{k+1} = shrink(\mathbf{y} - \hat{\mathbf{H}}\mathbf{x}^{k+1}, \frac{\lambda_2}{2}), \tag{12c}$$

$$\boldsymbol{\Theta}^{k+1} = \boldsymbol{\Theta}^k + \rho(\mathbf{z}^{k+1} - \mathbf{x}^{k+1}), \tag{12d}$$

where the shrinkage function is defined as

$$shrink(\omega, \tau) = \begin{cases} \omega - \tau & \omega > \tau \\ \omega + \tau & \omega < -\tau \\ 0 & otherwise. \end{cases} \tag{13}$$

The iteration is stopped when the difference between the objective functions of two successive iterations is less than a predefined threshold or the iteration number reaches the predefined maximum number.

Algorithm 1 Signal Recovery: ℓ_1-Minimization With ADMM

Input: $\hat{\mathbf{H}} \in \mathbb{R}^{N_R \times N_T}$, $\mathbf{y} \in \mathbb{R}^{\mathbf{N}_R \times 1}$, $iter_{max}$

Initializations: $\boldsymbol{\Theta}^0 \leftarrow \mathbf{0}$, $\mathbf{x}^0 \leftarrow \mathbf{0}$

for k=1... $iter_{max}$ **do**

$\mathbf{x}^{k+1} \leftarrow (2\hat{\mathbf{H}}^T\hat{\mathbf{H}} + \rho\mathbf{E})^{-1}(\rho\mathbf{z}^k + 2\hat{\mathbf{H}}^T(\mathbf{y} - \boldsymbol{\delta}^k) + \boldsymbol{\Theta}^k)$

$\mathbf{z}^{k+1} \leftarrow shrink(\mathbf{x}^{k+1} - \frac{\boldsymbol{\Theta}^k}{\rho}, \frac{\lambda_1}{\rho})$

$\boldsymbol{\delta}^{k+1} \leftarrow shrink(\mathbf{y} - \hat{\mathbf{H}}\mathbf{x}^{k+1}, \frac{\lambda_2}{2})$

$\boldsymbol{\Theta}^{k+1} \leftarrow \boldsymbol{\Theta}^k + \rho(\mathbf{z}^{k+1} - \mathbf{x}^{k+1})$

if $|\ \text{obj}^{k+1} - \text{obj}^k\ | \le \epsilon$ **then**

break

end if

end for

$\hat{\mathbf{x}} \leftarrow \mathbf{x}^{(k+1)}$

return $\hat{\mathbf{x}}$

Output: $\hat{\mathbf{x}} \in \mathbb{R}^{N_T \times 1}$

Remark 1: In this work, we specify the regularization multipliers λ_1 and λ_2 and penalty parameter ρ empirically. The effect of the multipliers and penalty parameter on the system performance is discussed in Section V. The optimum selection of λ_1, λ_2 and ρ is beyond the scope of this work, which will be considered in further researches.

However, the channel gain of the MIMO indoor VLC system is highly correlated in general, due to the system configuration including spatial positions of the transmitter (LEDs) and the receiver (PDs), inter-LED spacing, inter-PD spacing, radiation pattern of the LEDs, FOV of the PDs, etc. It may cause severe performance degradation. Although the transmitted signal can recovered by solving the ℓ_1-minimization problem under the assumption of the incomplete channel matrix, the property of the high-correlated VLC channel is unchanged, which may result in large sum-of-square error (SSE)[1] [36], especially with highly correlated channel, as Fig. 2 shown. In order to further improve the accuracy of the signal recovery, it is necessary to develop an approach that could reduce the channel coherence.

[1]The SSE is defined as $\|\mathbf{x} - \hat{\mathbf{x}}\|_F^2$, which is sensitive to the high coherence of channel.

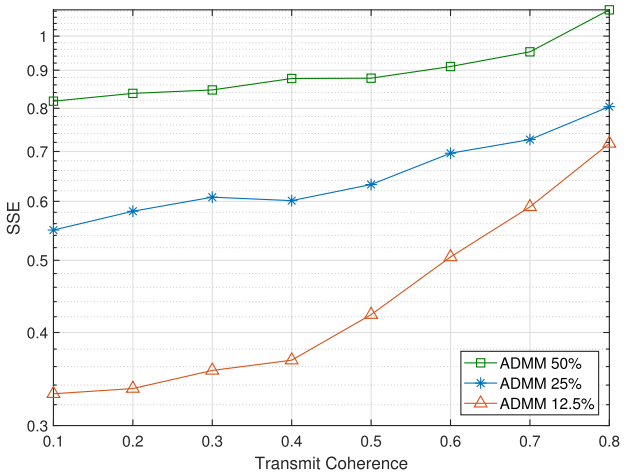

FIGURE 2. SSE against transmit coherence with different uncertainty rates (12.5%, 25%, 50%) under $N_T = N_R = 9$ MIMO configuration.

IV. COHERENCE-MINIMIZATION BEAMFORMING DESIGN

In CS theory, one of the fundamental mathematical problems is to recover signal vector accurately from equivalent sensing matrix. In order to understand the effect of channel coherence on signal recovery, we need to recall the definition of the *mutual coherence* [32]–[34], [37].

Definition ([32]): For a dictionary $\mathbf{D}$, its *mutual coherence* is defined as the largest absolute and normalized inner product between different columns in $\mathbf{D}$, that is,

$$\mu_m\{\mathbf{D}\} = \max_{1\le i,j\le k \text{ and } i\ne j} \frac{|\,\mathbf{d}_i^T\mathbf{d}_j\,|}{\|\mathbf{d}_i\|\|\mathbf{d}_j\|}\,. \tag{14}$$

It presents the worst similarity between the dictionary columns. Under the noiseless scenario, the signal $\mathbf{x}_0$ is guaranteed to be exactly recovered, once the inequality is satisfied [32]–[34], [37], that is,

$$\|\boldsymbol{\alpha}_0\|_0 < \frac{1}{2}\left(1+\frac{1}{\mu_m\{\mathbf{D}\}}\right)\,, \tag{15}$$

where the signal $\mathbf{x}_0$ has been constructed by $\mathbf{x}_0 = \mathbf{D}\boldsymbol{\alpha}_0$. It indicates that if the mutual coherence is as small as possible, a wider set of candidate signals are allowed with consequent of more accurate signal recovery.

Inspired by the above inequality and its hints behind, we strive to design the precoder matrix $\mathbf{W}$ under the noise case, in which the minimum mutual coherence of the equivalent sensing matrix $\left(\hat{\mathbf{H}}\mathbf{W}\right)$ can be achieved. However, it is difficult to compute the mutual coherence of the equivalent sensing matrix, especially when the number of transmit/receive antenna is large. Moreover, the mutual coherence represents the extreme pair-wise correlation between any two columns (atoms) which may lead to conservative performance [34], [37]. Therefore, considering that the recovery accuracy is more related to the average coherence [27], [37], we introduce the total coherence as an alternative coherence metric.

The incomplete channel $\hat{\mathbf{H}}$ can be rewritten as

$$\hat{\mathbf{H}} = \mathbf{U}_H\Lambda_H\mathbf{V}_H^H\,, \tag{16}$$

where $\mathbf{U}_H$ and $\mathbf{V}_H$ are the left and right unitary matrix, respectively, and Λ_H is the singular value matrix of $\hat{\mathbf{H}}$. At the transmit side, suppose $\Gamma = (\mathbf{W}^T\mathbf{V}_H^*)$, the total coherence $\mu(\Gamma)$ can be defined as

$$\mu(\Gamma) = \sum_{m=1}^{N_T}\sum_{n=1,n\ne m}^{N_T}\left(\Gamma(m)^H\Gamma(n)\right)^2\,. \tag{17}$$

In order to minimize the total coherence, we design the beamforming $\mathbf{W}$ to making the total coherence of the equivalent sensing matrix as close as possible to the identity matrix, that is,

$$\min_{\mathbf{W}}\ \|\mathbf{W}^T\mathbf{W}-\mathbf{I}_{N_T}\|_F^2\,, \tag{18a}$$

$$\text{s.t. } \|\mathbf{W}(n)\|_2^2 = 1,\quad n=1,\ldots,N_T, \tag{18b}$$

where the objective function can be further rewritten as

$$\begin{aligned}
&\|\Gamma^H\Gamma-\mathbf{I}_{N_T}\|_F^2\\
&= tr\left(\Gamma^H\Gamma\Gamma^H\Gamma-2\Gamma^H\Gamma+\mathbf{I}_{N_T}\right)\\
&= tr\left(\Gamma\Gamma^H\Gamma\Gamma^H-2\Gamma\Gamma^H+\mathbf{I}_L\right)+(N_T-L)\\
&\overset{(a)}{=} \|\Gamma\Gamma^H-\mathbf{I}_L\|_F^2+(N_T-L)\\
&= \|\mathbf{W}^T\mathbf{W}-\mathbf{I}_L\|_F^2+(N_T-L)\,,
\end{aligned} \tag{19}$$

with the equality (a) following from $\mathbf{V}_H\mathbf{V}_H^H = \mathbf{I}_{N_T}$. Note that, the computational complexing can be reduced significantly under the expression of (19), especially when the number of transmit antenna is large. However, the underlying problem is non-convex because of the individual power constraint on each beamforming (18b), which can be further relaxed as the sum of all the individual constraints, such as, $\sum_{n=1}^{L}\|\mathbf{W}(n)\|_2^2 = L$.

Proposition : The minimization of the total coherence in (18) can be achieved by

$$\min_{\mathbf{W}}\ \|\mathbf{W}^T\mathbf{W}-\mathbf{I}_L\|_F^2 \tag{20a}$$

$$\text{s.t. } \sum_{n=1}^{L}\|\mathbf{W}(n)\|_2^2 = L\,, \tag{20b}$$

with the optimum solution that is

$$\mathbf{W} = \mathbf{U}\left[\mathbf{I}_L, \mathbf{0}_{L,N_T-L}\right]^T\mathbf{V}^H, \tag{21}$$

where $\mathbf{U} \in \mathbb{C}^{N_t\times N_t}$ and $\mathbf{V} \in \mathbb{C}^{L\times L}$ are arbitrary unitary matrices.

Proof: Suppose the singular value decomposition (SVD) of $\mathbf{W} = \mathbf{U}_W\Lambda_W\mathbf{V}_W^H$ with the unitary matrices $\mathbf{U}_W \in \mathbb{C}^{N_t\times N_t}$ and $\mathbf{V}_W^H \in \mathbb{C}^{L\times L}$ and $\Lambda_W = [diag(\lambda_1,\ldots,\lambda_L)\ \mathbf{0}_{L,N_t-L})]^T$, the corresponding objective function can be rewritten as

$$\begin{aligned}
&\min_{\mathbf{W}}\quad \|\mathbf{W}^T\mathbf{W}-\mathbf{I}_L\|_F^2\\
&\quad = \min_{\lambda}\quad \|\mathbf{V}_W\Lambda_W^T\mathbf{U}_W^H\mathbf{U}_W\Lambda_W\mathbf{V}_W^H-\mathbf{I}_L\|_F^2
\end{aligned}$$

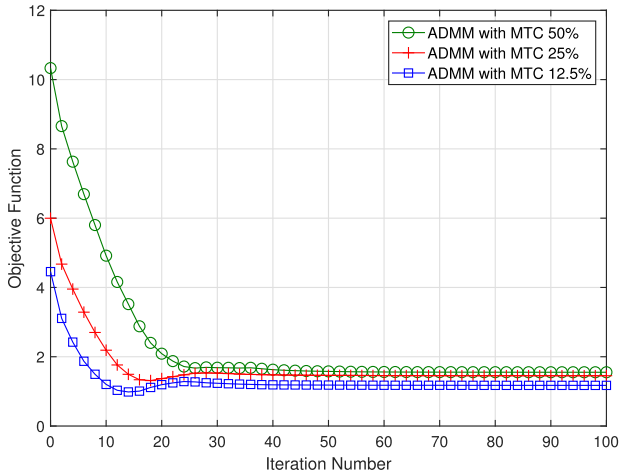

FIGURE 3. Convergence under varied missing rates (12.5%, 25%, 50%).

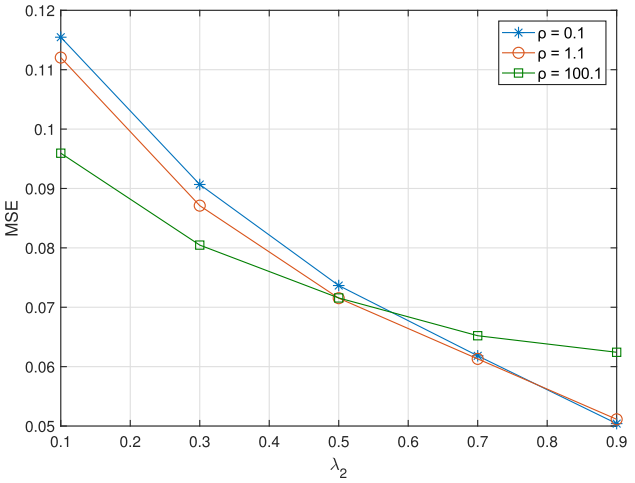

FIGURE 4. Effect of parameter selection on MSE performance.

$$
\begin{aligned}
&= \min_{\lambda} \quad \|\mathbf{V}_W(\Lambda_W^T\Lambda_W - \mathbf{I}_L)\mathbf{V}_W^H\|_F^2 \\
&= \min_{\lambda} \quad \|\Lambda_W^T\Lambda_W - \mathbf{I}_L\|_F^2 \\
&= \min_{\lambda} \quad \sum_{n=1}^{L}(\lambda_n^2 - 1)^2. \qquad (22)
\end{aligned}
$$

As the result, the underlying problem now can be expressed as

$$\min_{\lambda} \ \sum_{n=1}^{L}(\lambda_n^2 - 1)^2 \qquad (23a)$$

$$\text{s.t.} \ \sum_{n=1}^{L}\lambda_n^2 = L\,. \qquad (23b)$$

The corresponding Lagrangian function can be presented as

$$\mathcal{L}(\lambda^2, \varsigma) = \sum_{n=1}^{L}(\lambda_n^2 - 1)^2 + \varsigma(\sum_{n=1}^{L}\lambda_n^2 - L)\,, \qquad (24)$$

in which the optimum solution λ_n^2 can be achieved by solving

$$\frac{\partial\mathcal{L}(\lambda^2, \varsigma)}{\partial\lambda} = 0\,, \qquad (25)$$

$$2\lambda_n^2 + \varsigma - 2 = 0\,, \qquad (26)$$

that is, $\lambda_n^2 = 1,\ \forall n$. Therefore, the optimal $\mathbf{W}$ can be achieved as (21) with the optimal matrix $\Lambda_W = \left[\mathbf{I}_L, \mathbf{0}_{N_T-L}\right]^T$. □

Remark 2: The optimum solution (21) indicates that any unitary $\mathbf{U}$ and $\mathbf{V}$ with the optimum singular values can minimize the total coherence. Later in the simulations, it shows that the system performance can be improved significantly after minimizing the total coherence.

Remark 3: The proposed beamforming minimizes the mutual coherence without requiring CSI or the backhaul links, which is compatible with the features of the propagation of the VLC.

V. SIMULATION

In this work, we consider a typical $5 \times 5 \times 5\ m^3$ room which is composed of 2 LED arrays. Each LED array with 4 LEDs is uniformly distributed over the entire surface of the ceiling with 1m spacing. The receivers with 2×4 PDs are placed at a height of 1m with 0.1m separation. The proposed ℓ_1-minimization via ADMM with minimum total coherence (abbr. as ADMM with MTC) is compared to the ℓ_1-minimization via ADMM with zero-forcing beamforming (abbr. as ADMM with ZF) [31], the ℓ_1-minimization via ADMM with SVD beamforming (abbr. as ADMM with SVD) [28], the ℓ_1-minimization via ADMM without beamforming design (8) (abbr. as ADMM), the ℓ_1-minimization via FISTA without beamforming (abbr. as FISTA) [38]. Moreover, the parameters λ_1, λ_2, ρ and ϵ are set to be $\lambda_1 = 0.3$, $\lambda_2 = 0.7$, $\rho = 1.1$, and $\epsilon = 10^{-4}$, respectively. Except Fig. 7, the rest of all figures are under the system configuration with $N_T = N_R = 8$. Note that, the line-missing case is considered in the following simulations.

A. CONVERGENCE, PARAMETER SELECTION AND COHERENCE EFFECT

The proposed algorithm is designed to minimize the transmit coherence and improve the system performance. Before demonstrating its effectiveness, the convergence and effect of the transmit coherence are explored first. Fig.3 illustrates the convergence of the proposed algorithm with varied missing rate under SNR = 15dB, in which the proposed design can converge monotonically within a few iterations. Moreover, the missing rate may slow down the convergence speed, since the iteration number becomes large when the missing rate increases. It is worth to note that the high missing rate however has limited effect on the achievable value of the objective function.

Fig.4 illustrates the effect of the selection of regularization multipliers and penalty parameter on mean square error (MSE) performance where SNR = 15dB and missing rate is 25%. The MSE is followed the definition in [36],

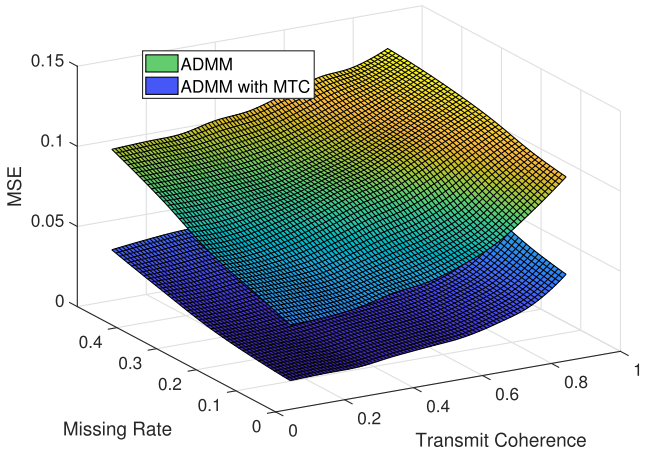

FIGURE 5. MSE performance versus transmit coherence and missing rate.

that is,

$$\text{MSE} = \frac{1}{N_T}\|\mathbf{x} - \hat{\mathbf{x}}\|_F^2 .$$

It shows the different combination of λ_1, λ_2 and ρ results in varied MSE. The combination of either small λ_2 and high ρ or large λ_2 and small ρ can achieve the low MSE. The best combination of λ_1, λ_2 and ρ will be discussed in our further research.

Furthermore, we investigate the effect of the transmit coherence and missing rate on the MSE performance which is presented in three-dimensional space with SNR= 15dB, shown in Fig.5. It shows that the obtained MSE value increases slowly as long as the increased transmit coherence and missing rate, which demonstrates that the proposed ADMM with MTC outperforms that without beamforming design. It is because that the MTC beamforming design can reduce the transmit coherence significantly. Moreover, the effect of the transmit coherence on all mentioned algorithms with SNR = 15dB and 50% missing rate is presented in Fig.6. It shows that the beamforming framework, including ZF, SVD and MTC, can provide further improvement on the signal recovery. More specifically, the ADMM with MTC achieves the lowest MSE compared with other schemes, even the transmit coherence arrives to 0.8. Moreover, the ADMM with MTC is not sensitive to the increased transmit coherence, which indicates that the proposed algorithm can effectively reduce the effect of the transmit coherence on the signal recovery.

B. EFFECTIVENESS OF PROPOSED BEAMFORMING DESIGN

The effectiveness of the proposed design is further demonstrated in terms of MSE and bit error rate (BER) performance, shown in Fig.7, Fig.8 and Fig. 9, respectively. Fig.7 explores the sensitivity of the achieved MSE under different MIMO configurations, that is, (8 × 8 and 16 × 16) with SNR = 15dB. When the missing rate grows, all the MSEs obtained by aforementioned designs increase. Because of the transmit coherence reduction by the proposed

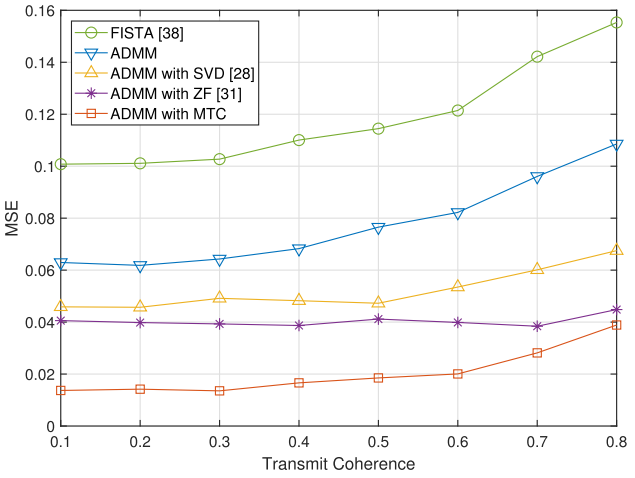

FIGURE 6. MSE performance versus transmit coherence.

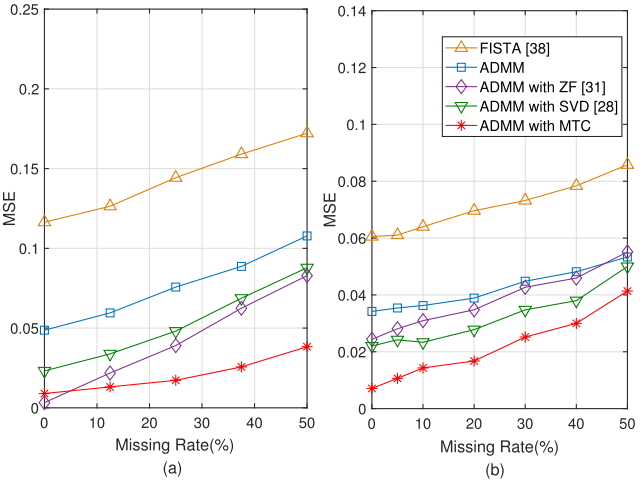

FIGURE 7. MSE performance under different system configurations (a) 8 × 8, (b) 16 × 16 MIMO.

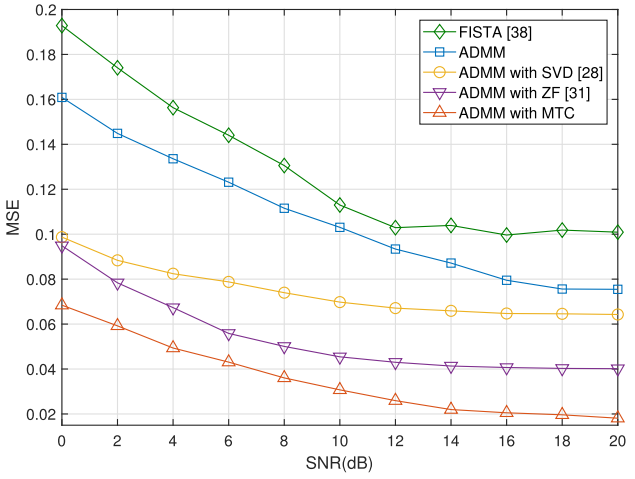

FIGURE 8. MSE performance versus SNR.

beamforming, the ADMM with MTC significantly improves the MSE performance which provides the lowest MSE, followed by ADMM with SVD and ADMM with ZF. Moreover,

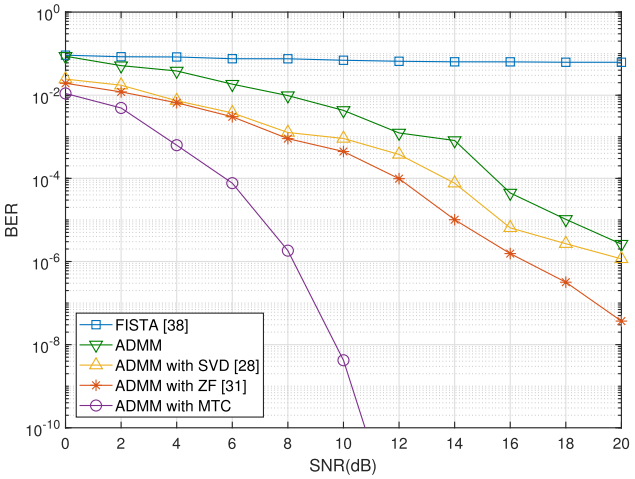

FIGURE 9. BER performance versus SNR.

as the MIMO size increases, the impacts of the channel missing rate on MSE performances become negligible, and the gap among all mentioned algorithms becomes narrow. It means that, the small scale MIMO system can earn benefits on the proposed ADMM with MTC scheme, which becomes less considerable as the MIMO size increases.

Fig.8 demonstrates MSE performance versus signal-to-noise ratio (SNR) under 25% missing rate. As we expected, the MSE value decreases with increasing SNR. The ADMM with MTC achieves lowest MSE over all SNR region, which is much lower than that achieved by ADMM approach. Moreover, the difference between ADMM with ZF and ADMM with SVD is small in the low SNR, which becomes significant as the SNR increases.

The BER performance with 25% missing rate is illustrated in Fig.9. With the increased SNR, the BER performance monotonously decreases, where ADMM with beamforming schemes achieve lower BER while FISTA algorithm provides the highest BER. It indicates that the beamforming framework can significantly improve the accuracy of the signal recovery. Compared with the ZF and SVD beamforming schemes, the proposed MTC beamforming scheme can effectively reduce the transmit coherence, and obtain the lowest BER among all mentioned schemes.

VI. CONCLUSION

In this paper, we consider the indoor MIMO VLC system with random shadowing effect. Due to the blockages of the transmit links caused by the shadowing, we model the channel as incomplete matrix with sparse missing elements, and reconstruct the transmitted signal by the $\ell_1 - \ell_1$ minimization in which the optimum solutions are achieved via ADMM algorithm iteratively. Considering that the high coherence of the indoor VLC channel might degrade the performance of the signal recovery, we further develop the beamforming design to reduce the total coherence. Simulation results validate that the proposed ℓ_1-minimization with ADMM can improve the performance of the signal recovery and the developed MTC beamforming can further enhance the accuracy of the signal recovery.

REFERENCES

[1] S. Wu, H. Wang, and C. H. Youn, "Visible light communications for 5G wireless networking systems: From fixed to mobile communications," *IEEE Netw.*, vol. 28, no. 6, pp. 41–45, Nov. 2014.

[2] Z. Zeng, H. Du, and Z. Wu, "Min-max-MSE transceiver design for MU-MIMO VLC system," *Wireless Commun. Mobile Comput.*, vol. 2018, Apr. 2018, Art. no. 3080643.

[3] S. Jivkova and M. Kavehrad, "Shadowing and blockage in indoor optical wireless communications," in *Proc. GLOBECOM*, Dec. 2003, pp. 3269–3273.

[4] T. Komine and M. Nakagawa, "A study of shadowing on indoor visible-light wireless communication utilizing plural white LED lightings," in *Proc. ISWCS*, Sep. 2004, pp. 36–40.

[5] P. Chvojka, S. Zvanovec, P. A. Haigh, and Z. Ghassemlooy, "Channel characteristics of visible light communications within dynamic indoor environment," *J. Lightw. Technol.*, vol. 33, no. 9, pp. 1719–1725, May 1, 2015.

[6] H. Farahneh, C. Mekhiel, A. Khalifeh, W. Farjow, and X. Fernando, "Shadowing effects on visible light communication channels," in *Proc. CCECE*, May 2016, pp. 1–5.

[7] Y. Xiang, M. Zhang, M. Kavehrad, C. Sakib, M. Liu, J. Wu, and X. Tang, "Human shadowing effect on indoor visible light communications channel characteristics," *Opt. Eng.*, vol. 53, p. 086113, Aug. 2014.

[8] Z. Dong, T. Shang, Y. Gao, and Q. Li, "Study on VLC channel modeling under random shadowing," *IEEE Photon. J.*, vol. 9, no. 6, pp. 1–16, Dec. 2017.

[9] X. Nan, P. Wang, L. Guo, L. Huang, and Z. Liu, "A novel VLC channel model based on beam steering considering the impact of obstacle," *IEEE Commun. Lett.*, vol. 23, no. 6, pp. 1003–1007, Jun. 2019.

[10] W. Zhang, M. I. S. Chowdhury, and M. Kavehrad, "Asynchronous indoor positioning system based on visible light communications," *Opt. Eng.*, vol. 53, no. 4, pp. 1–10, 2014.

[11] Z. Vatansever and M. Brandt-Pearce, "Effects of unknown shadowing and non-line-of-sight on indoor tracking using visible light," in *Proc. MILCOM*, Oct. 2017, pp. 501–506.

[12] H. Marshoud, D. Dawoud, V. M. Kapinas, G. K. Karagiannidis, S. Muhaidat, and B. Sharif, "MU-MIMO precoding for VLC with imperfect CSI," in *Proc. IWOW*, Sep. 2015, pp. 93–97.

[13] H. Ma, L. Lampe, and S. Hranilovic, "Coordinated broadcasting for multiuser indoor visible light communication systems," *IEEE Trans. Commun.*, vol. 63, no. 9, pp. 3313–3324, Sep. 2015.

[14] Z.-G. Sun, H.-Y. Yu, W.-C. Li, Z.-J. Tian, and Y.-J. Zhu, "Power-efficient linear precoding for MU-MISO VLC systems with channel uncertainty," *IEEE Photon. Technol. Lett.*, vol. 30, no. 7, pp. 626–629, Apr. 1, 2018.

[15] N. Vucic, H. Boche, and S. Shi, "Robust transceiver optimization in downlink multiuser MIMO systems," *IEEE Trans. Signal Process.*, vol. 57, no. 9, pp. 3576–3587, Sep. 2009.

[16] H. Sifaou, A. Kammoun, K. Park, and M. Alouini, "Robust transceivers design for multi-stream multi-user MIMO visible light communication," *IEEE Access*, vol. 5, pp. 26387–26399, 2017.

[17] M. Di Renzo, D. De Leonardis, F. Graziosi, and H. Haas, "Space shift keying (SSK—) MIMO with practical channel estimates," *IEEE Trans. Commun.*, vol. 60, no. 4, pp. 998–1012, Apr. 2012.

[18] W. O. Popoola, E. Poves, and H. Haas, "Error performance of generalized space shift keying for indoor visible light communications," *IEEE Trans. Commun.*, vol. 61, no. 5, pp. 1968–1976, May 2013.

[19] M. Di Renzo, H. Haas, A. Ghrayeb, S. Sugiura, and L. Hanzo, "Spatial modulation for generalized MIMO: Challenges, opportunities, and implementation," *Proc. IEEE*, vol. 102, no. 1, pp. 56–103, Jan. 2014.

[20] C. R. Kumar and R. K. Jeyachitra, "Dual-mode generalized spatial modulation MIMO for visible light communications," *IEEE Commun. Lett.*, vol. 22, no. 2, pp. 280–283, Feb. 2018.

[21] C. R. Kumar and R. K. Jeyachitra, "Improved joint generalized spatial modulations for MIMO-VLC systems," *IEEE Commun. Lett.*, vol. 22, no. 11, pp. 2226–2229, Nov. 2018.

[22] T. Kang and R. A. Iltis, "Matching pursuits channel estimation for an underwater acoustic OFDM modem," in *Proc. ICASSP*, Mar. 2008, pp. 5296–5299.

[23] G. Z. Karabulut and A. Yongacoglu, "Sparse channel estimation using orthogonal matching pursuit algorithm," in *Proc. IEEE 60th Veh. Technol. Conf. (VTC-Fall)*, vol. 6, Sep. 2004, pp. 3880–3884.
[24] G. Taubock, F. Hlawatsch, D. Eiwen, and H. Rauhut, "Compressive estimation of doubly selective channels in multicarrier systems: Leakage effects and sparsity-enhancing processing," *IEEE J. Sel. Topics Signal Process.*, vol. 4, no. 2, pp. 255–271, Apr. 2010.
[25] X. Quan, X. Jing, S. Sun, H. Huang, and L. Wang, "Sparse channel estimation in OFDM systems using improved smooth ℓ_0 algorithm," in *Proc. ISCIT*, Sep. 2014, pp. 346–350.
[26] T. Chen, L. Liu, B. Tu, Z. Zheng, and W. Hu, "High-spatial-diversity imaging receiver using fisheye lens for indoor MIMO VLCs," *IEEE Photon. Technol. Lett.*, vol. 26, no. 22, pp. 2260–2263, Nov. 15, 2014.
[27] A. K. Gupta and A. Chockalingam, "Performance of MIMO modulation schemes with imaging receivers in visible light communication," *J. Lightw. Technol.*, vol. 36, no. 10, pp. 1912–1927, May 15, 2018.
[28] Q. Liu, S. Xiao, K. Huang, and Z. Zhong, "A SVD-based optical MIMO precoding scheme in indoor visible light communication," *Int. J. Future Comput. Commun.*, vol. 3, no. 6, pp. 421–426, 2014.
[29] Q. Wang, Z. Wang, and L. Dai, "Multiuser MIMO-OFDM for visible light communications," *IEEE Photon. J.*, vol. 7, no. 6, pp. 1–11, Dec. 2015.
[30] H. Marshoud, P. C. Sofotasios, S. Muhaidat, B. S. Sharif, and G. K. Karagiannidis, "Optical adaptive precoding for visible light communications," *IEEE Access*, vol. 6, pp. 22121–22130, 2018.
[31] Y. Fan, Q. Zhao, B. Kang, and L. Deng, "Equivalent ZF precoding scheme for downlink indoor MU-MIMO VLC systems," *Opt. Commun.*, vol. 47, pp. 402–409, Jan. 2018.
[32] V. Abolghasemi, S. Ferdowsi, B. Makkiabadi, and S. Sanei, "On optimization of the measurement matrix for compressive sensing," in *Proc. 18th Eur. Signal Process. Conf.*, Aug. 2010, pp. 427–431.
[33] L. Zelnik-Manor, K. Rosenblum, and Y. C. Eldar, "Sensing matrix optimization for block-sparse decoding," *IEEE Trans. Signal Process.*, vol. 59, no. 9, pp. 4300–4312, Sep. 2011.
[34] R. Obermeier and J. A. Martinez-Lorenzo, "Sensing matrix design via mutual coherence minimization for electromagnetic compressive imaging applications," *IEEE Trans. Comput. Imag.*, vol. 3, no. 2, pp. 217–229, Jun. 2017.
[35] S. Khanna and C. R. Murthy, "Decentralized joint-sparse signal recovery: A sparse Bayesian learning approach," *IEEE Trans. Signal Inf. Process. Netw.*, vol. 3, no. 1, pp. 29–45, Mar. 2017.
[36] A. S. Jagtap, R. Shriram, and H. T. Patil, "Comparison of decomposition and reconstruction of 2D signal using slantlet transform and DCT," in *Proc. ICCSP*, Apr. 2017, pp. 0593–0597.
[37] G. Li, Z. Zhu, D. Yang, L. Chang, and H. Bai, "On projection matrix optimization for compressive sensing systems," *IEEE Trans. Signal Process.*, vol. 61, no. 11, pp. 2887–2898, Jun. 2013.
[38] T. Oishi and Y. Kuroki, "An $\ell_1 - \ell_1$-norm minimization solution using ADMM with FISTA," in *Proc. ICIIBMS*, Oct. 2018, pp. 200–203.

HUIQIN DU (M'10) received the B.Sc. degree in electronic information science and technology from the Beijing University of Chemical Technology, China, in 2004, the M.Sc. degree (Hons.) in radio frequency communication system from the University of Southampton, in 2006, and the Ph.D. degree in signal processing from The University of Edinburgh, in 2010. From 2010 to 2013, she was a Research Fellow with Queen's University Belfast and The University of Edinburgh. Since 2013, she has been with the College of Information Science and Technology, Jinan University, Guangdong, China, as an Associate Professor. Her current research interests include statistical signal processing, visible light communication, wireless MIMO communications, cognitive radio networks, massive MIMO, and hybrid beamforming.

CHONG ZHANG received the B.S. degree in electronics and information engineering from the College of Information Science and Technology, Jinan University, Guangdong, China, in 2017, where she is currently pursuing the M.S. degree. Her current research interest includes signal recovery in visible light communications.

ZUJIAN WU received the B.Sc. degree in computer science and technology from the Harbin University of Science and Technology, China, in 2004, the M.Sc. degree in computer application technology from Central South University, China, in 2008, and the Ph.D. degree in information systems and computing from Brunel University, U.K., in 2013. He was sent to Brunel University to pursue the Ph.D. degree by the China Scholarship Council (CSC), in 2008, under the program of Construction of High Level Universities. He was a Research Fellow with the School of Natural and Computing Science, Aberdeen University, U.K. He was with an International Research Team in the project CRISP supported by the U.K. BBSRC. He was in charge of qualitatively modeling response signaling pathways of fungi biochemical systems based on the artificial intelligence and optimization algorithms. He joined Jinan University as a Lecturer, in 2013, and was promoted to Associate Professor, in 2018. His research interests include artificial intelligence, optimization algorithms, data mining, and systems biology.